Energy Neutral Activity Monitoring: Wearables Powered by Smart Inductive Charging Surfaces

Xenofon Fafoutis*, Lindsay Clare*, Neil Grabham†, Steve Beeby†,
Bernard Stark*, Robert Piechocki* and Ian Craddock*
*Department of Electrical and Electronic Engineering
University of Bristol, UK
{xenofon.fafoutis, aelrc, bernard.stark, r.j.piechocki, ian.craddock}@bristol.ac.uk
†Electronics and Computer Science
University of Southampton, UK
{njg, spb}@ecs.soton.ac.uk

***Abstract*—Wearable technologies play a key role in the shift of traditional healthcare services towards eHealth and self-monitoring. Maintenance overheads, such as regular battery recharging, impose a limitation on the applicability of such technologies in some groups of the population. In this paper, we propose an activity monitoring system that is based on wearable sensors that are powered by textile inductive charging surfaces. By strategically positioning these surfaces on pieces of furniture that are routinely used, the system passively charges the wearable sensor whilst the user is present. As a proof-of-concept example, experiments conducted on a prototype implementation of the system suggest that 36 minutes of daily desktop computer usage are on average sufficient to maintain a wearable sensor energy neutral.**

***Index Terms*—Wearable Technologies; Inductive Power Transfer; Energy Neutral Operation; Energy Harvesting; eHealth; Internet of Things**

I. Introduction

Modern healthcare is challenged by trends of increasing ageing populations and chronic illness. There is therefore a drive to develop sensing technologies, to encourage people to manage their own well-being at home. It has been shown that healthcare provision in the comfort of a home leads to improved outcomes in some medical procedures, and maintains the dignity and independence of the elderly [1]. In addition, home care can provide cost-effective prevention of mental health conditions [2]. Emerging digital technologies, investigated in the context of smart homes [3][4] and the Internet of Things (IoT), provide the necessary infrastructure to support this paradigm shift in healthcare provision.

Activity monitors, such as Fitbit, Jawbone UP and Nike+ Fuelband SE, have recently appeared in the consumer electronics market [5]. These wearable gadgets demonstrate the rise of a trend towards self-monitoring, as well as the user acceptability of wearable technologies [6]. However, such gadgets are of limited use for medical applications due to the limited accessibility of the raw data, their lack of interoperability with other healthcare systems and their limited expandability to new sensor technologies. Furthermore, their need for regular recharging (typical battery lifetime of less than a week) hinders their suitability for target groups where sensing should be unobtrusive and fully automated, such as people with mild cognitive impairments. Regular recharging reduces the effectiveness of wearable technologies even in the general population, as every time a wearable sensor is removed to be charged, there is a loss of data, and the inconvenience of recharging the sensor brings the risk of reduced usage.

A promising direction towards maintenance-free wearable technologies is energy harvesting [7]. Energy harvesting implies the use of energy sources that already exist in the surrounding environment, such as light [8] and vibrations [9]. Another approach, that increases the power density of the receiver, is to wirelessly charge devices using deliberate wireless power sources, for example inductive charger pads, or RF carrier-wave transmitters. Standards have therefore been developed to facilitate the charging of multiple sensors from standardised transmitters. Qi, for instance, is an inductive power standard that implements wireless contact charging [10]. Despite being wireless, Qi-devices require user interaction, as they need to be placed directly onto a Qi charger pad.

An additional challenge of these battery-less powering techniques are the low received power levels. Indeed, most ambient energy sources are limited [11], whilst wireless power transfer technologies are typically characterised by very low efficiencies [12]. As a result, the wireless sensor and its power management are typically required to operate on mW or lower power budgets, and energy efficiency becomes a vital system requirement. According to the Energy Neutral Operation (ENO) principle [13], a node is sustainable if, over a time period that its energy buffers can support, the consumed energy is less than or equal to the harvested energy. Therefore, providing ENO is a twofold research challenge: harvested energy needs to be maximised and energy consumption needs to be minimised.

In this paper, we present an unobtrusively recharging wearable sensing system. Different to Qi-compliant devices, the inductive chargers are distributed over frequently-used rigid and soft furniture, to create an extended-range charging zone that does not require contact or deliberate placement of the receiver, thus providing ENO. Using the wireless communication channel, normally used for relaying the sensor data,

the smart charging surfaces detect when the user is in close proximity and when the wearable device requires charging. As a proof of concept, we focus on a smart charging desk, evaluating how frequently a user needs to use their computer for the wearable to be energy neutral.

The remainder of the paper is organised as follows. Section II provides background on medium-range inductive charging and summarises the related work. Section III documents the system design: wearable sensor (Section III-A) and smart infrastructure (Section III-B). Section IV evaluates the system, identifying the requirements for ENO. Finally, Section V summarises the paper providing final remarks.

II. Medium-Range Inductive Power Transfer

The smart charging surfaces, employed to sustain a wearable monitoring device, are based on inductive power transfer (IPT). Fig. 1 shows the basic components of an IPT system. An alternating current provided by a driver circuit flows through a transmit coil; this results in an alternating flux around the coil, which links with the turns of the receive coil, inducing a voltage into it, in accordance with Faradays law. The end-platform will normally require a stable DC (Direct Current) voltage to power electronic circuits, but the induced voltage is alternating, and will vary in amplitude with the relative positioning of the coils, therefore a stage of power-conditioning, incorporating rectification and voltage regulation, is required. An IPT system operates on the same principle as a conventional transformer, the difference being that whereas the transformer windings are tightly coupled, sharing a common flux path around a high permeability magnetic core, coupling for the IPT system is through air, having a much lower permeability; that of free space. For coupled magnetic circuits, the coupling factor k is

$$k = \frac{V_{SEC}}{V_{PRI}} \sqrt{\frac{L_P}{L_S}} \ , \tag{1}$$

where V_{PRI} is an alternating voltage applied to one coil and V_{SEC} is the voltage induced into the other coil, and L_P and L_S refer to the inductance of the primary and secondary coils respectively. For a typical iron-cored transformer, k will be well over 0.9, but IPT systems may operate with k as low as 0.01. It is this large difference in k which forces the designer of an IPT system to adopt more complicated arrangements for both primary and secondary circuits, as compared to the straightforward supply and load connections of a conventional transformer. Both primary and secondary circuits are normally made to be resonant at the same frequency: in the case of the primary, this reduces the Volt-Amperes required from the driver, as it only has to supply the real part of the power. Operating the receive circuit in resonance has the effect of magnifying the voltage developed across the coil, from just the induced voltage, to the induced voltage multiplied by the quality factor of the tuned circuit. From a physical point of view, a coil at resonance situated in a weak magnetic field has the effect of concentrating the magnetic flux around it. Tuning the receive circuit therefore somewhat compensates

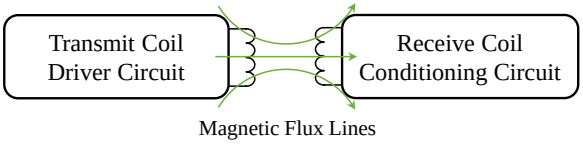

Fig. 1. Basis for an IPT system.

for the loose coupling typical of most IPT systems, greatly increasing the power available when the coils are spaced widely or misaligned.

IPT traces its roots to Nikola Tesla, over a hundred years ago, for electrical power transmission without wires [14]. The uses of IPT cover a wide range of applications and power levels, from multi-kilowatt electric vehicle charging systems [15] to medical implants at milliwatt levels as in [16] and [17], which describe inductive powering of a cortical implant and a retinal implant respectively. In [18], the use of IPT for mobile wearable medical devices is dealt with, including the issue of human exposure limits, and in [19], inductive powering of a wireless monitoring suit for children in hospital is described. Other examples of IPT applied to wearables are to be found in [20] and [21]. [22] and [23] give special attention to the design of IPT systems that conform to European ICNIRP 1998 human exposure guidelines. Most IPT systems, including the Qi inductive power standard [10], operate at close range, as in toothbrush chargers and more recently, charging pads for mobile phones, where the device to be charged is either slotted into the charger, or must be a maximum of 1 cm above it. In this work we present an experimental extended-range IPT system, where the vertical separation can be up to 20 cm, and the range is extended laterally using resonant repeater coils.

III. System Design

The system focuses on residential monitoring in a smart home. It is composed of an ultra-low energy wearable activity sensor and multiple receiver units, as summarised in in Fig. 2. Energy-efficient communication is achieved through a broadcasting network that relies on Bluetooth Low Energy (BLE) [24] for wireless communication. The receiver units are co-located with smart inductive charging surfaces. Using textile transmit coils, the wearable sensor can be charged whilst being in the vicinity of the charging surface. Textile coils, strategically placed in furniture regularly used during the daily routine; for example a dining table, the armrests of a sofa, or a desk; allow the wearable sensor to be charged whilst in the vicinity of the charging surface, thereby providing a passive charging solution that does not require any action from the user. Using information encoded in the BLE packets and the Received Signal Strength Indicator (RSSI), the smart charging surface is able to detect when the user is in close proximity and when the wearable requires charging, activating itself only when necessary. The principle idea is that users regularly visit such furniture throughout the course of a day, providing sufficient time to recharge the energy storage unit of their wearable device.

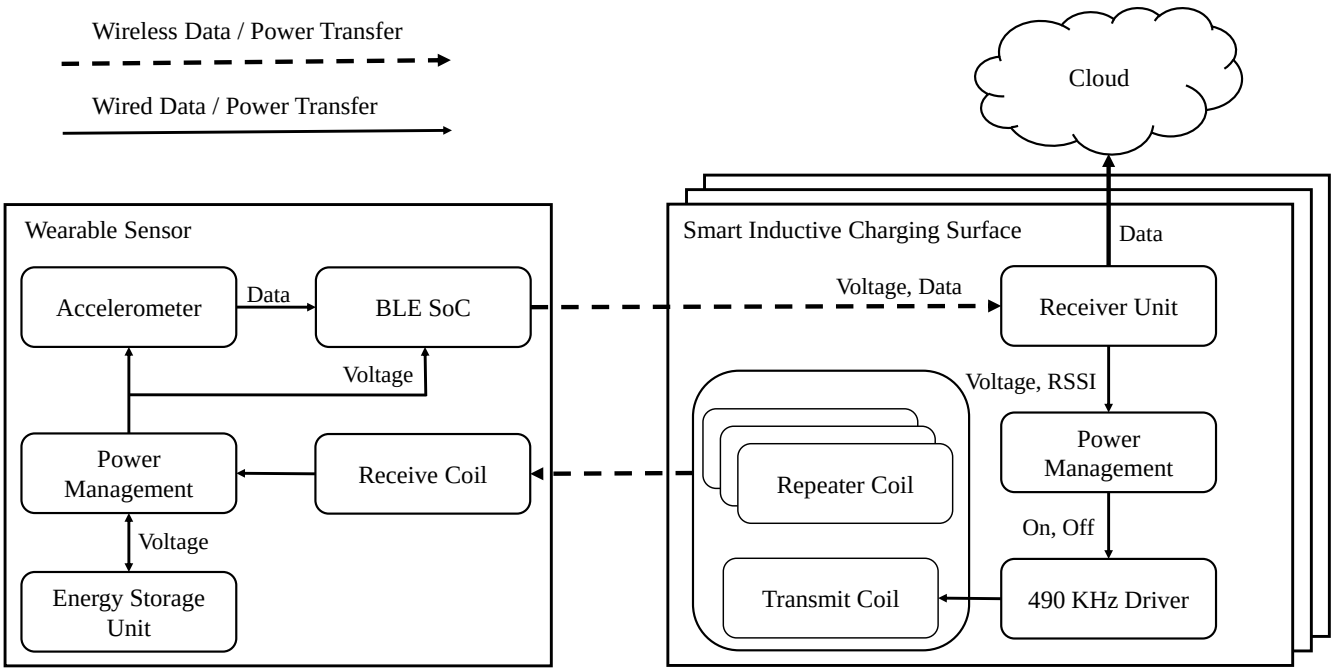

Fig. 2. System overview.

A. Wearable Sensor

User acceptance constitutes the primary requirement when designing wearable sensors. Such requirement introduces several challenges in the hardware and firmware design. Indeed, the requirement for wearable sensors to be lightweight and low-profile, introduces several constraints in the size of the employed antenna, the IPT circuitry, and energy storage unit.

The presented prototype, shown in Fig. 3, is based on a custom wearable activity monitoring board. It is an accelerometer-based sensor that relies on Bluetooth Low Energy (BLE) for wireless communications. The dimensions of the printed circuit board (PCB) are $24 \times 39 \times 3.8$ mm. The core component is an nRF51822 system-on-chip (SoC) [25] which incorporates an ARM Cortex™ M0 micro-controller unit (MCU), 32KB of RAM, 256KB of non-volatile flash memory, and a BLE radio. The employed accelerometer is the ADXL362, interfaced to the main core over SPI (Serial Peripheral Interface). The ADXL362 is a micro-power 3-axis digital accelerometer that has 12-bit resolution, a maximum sampling frequency of 400 Hz, and supports measurement ranges of $\pm$2g, $\pm$4g, $\pm$8g. It also employs a 512-sample FIFO buffer (First In First Out).

Ultra-low power consumption is partially achieved by operating the nRF51822 at 1.8 V. The system employs the LTC3388 DCDC (Direct Current to Direct Current) converter that efficiently converts any voltage source from 2.7 V to 6 V, to the required 1.8 V. In the prototype shown in Fig. 3, a 330 mF supercapacitor is employed as the energy storage unit. The board also employs an MCP73831, a 500 mA linear charge management controller with 4.2 V output that is compatible with single cell 3.7 V Li-Po batteries. The

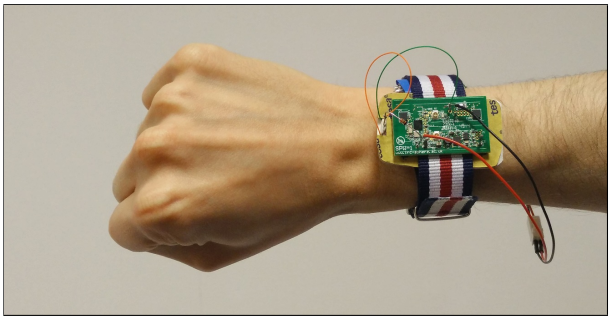

Fig. 3. The wearable sensor prototype.

MCP73831 is, by default, isolated from the remainder of the circuit and can be optionally connected. Energy awareness is also considered in the design. With a potential divider, the high voltage of the source is appropriately conditioned to the requirements of the nRF51822's analog-to-digital converter (ADC). A transistor switch guarantees nA current consumption by the potential divider when the feature is not used.

With regard to the IPT circuitry, the receive coil circuit fits inside one half of the wearable enclosure which has inside dimensions of 25×47 mm. The voltage induced into a coil due to a changing magnetic field is proportional to the turn-area product, and therefore to take maximum advantage of this, the maximum number of turns are placed around the periphery of the enclosure, as shown in Fig. 4 (left), which shows the receive coil with the parallel-connected tuning capacitors. The coil uses 10 turns of $36/0.04$ mm Litz wire, and when the unit is assembled, a flexible ferrite backing shields it from the

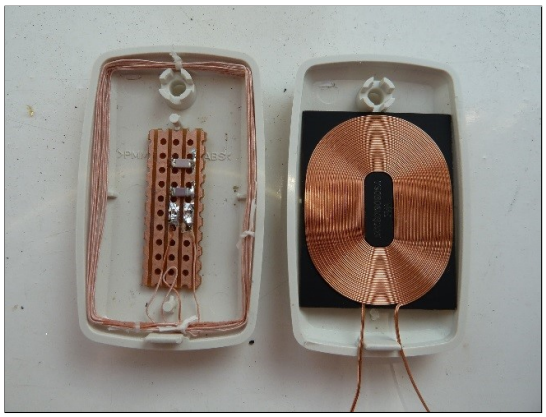

Fig. 4. Receive coil inside wearable enclosure with tuning capacitors (left). Commercial coil intended for Qi-compliant short-range IPT (right). This has similar inductance but lower coupling factor, and hence lower mutual inductance to the primary coil.

ground-plane and, most importantly, the RF circuitry of the board. A commercial ferrite-backed coil intended for short-range Qi-compliant IPT systems also fits neatly into the case, as seen in Fig. 4 (right), but is less effective in this application, having a turn-area product 0.6 that of the Litz coil. The tuning capacitor must fit within the available space, yet have low equivalent series resistance (ESR), if the Q of the resonant circuit is to approach that of the native Q of the coil, in this case 46. Combinations of capacitors in parallel were used to tune as close as possible to the operating frequency of 490 KHz.

The voltage developed across the receive-coil is half-wave rectified; this saves a diode forward drop compared to a bridge circuit , whilst causing only slight distortion to the coil current waveform. The rectifier is fed from a centre-tap on the coil; this is done to give a better match between the optimum load of the tuned-circuit and the load presented by the rectifier. A shunt regulator limits the voltage to 5.5 V, the maximum terminal voltage for a supercapacitor, which serves the role of the energy storage unit.

This simple power-conditioning circuit was chosen for its ability to fit easily into the space available; a better match to the resonant circuit is possible using a micro-power flyback converter operating in discontinuous inductor current mode, which may be adjusted to emulate the optimum load resistance of the resonant circuit, whilst transferring power to a variable load [26]. Tests showed that when using this scheme, the range of operation vertically above the transmit coil was increased by approximately 20%. However, further work on miniaturisation is needed to allow it to fit into a low-profile wearable enclosure.

As far as wireless communications are concerned, the wearable sensor employs a loop antenna printed on the FR4 substrate, matched to the differential RF output of the nRF51822. The loop antenna was measured to have an efficiency of about 60% (relative to a high-efficiency reference antenna) and a maximum directivity of about 7 dBi (computed from the measured 3D radiation pattern). The antenna was measured in isolation in an anechoic chamber. The BLE radio of the nRF51822 supports 7 transmission power levels ranging from -20 dBm to 4 dBm with a step of 4 dB.

According to the BLE specifications [24], a device can operate in either of four distinct roles, namely *Broadcaster*, *Observer*, *Peripheral*, and *Central*. The two former roles are based on a connectionless unidirectional communication model where the *Broadcaster* is the transmitter and the *Observer* is the receiver. The two latter roles are based on a connection-oriented model, where the *Central* is the master and the *Peripheral* is the slave. Focusing on long-term residential monitoring, we opt for the connectionless communication model, in which the wearable device acts as a *Broadcaster*. The connectionless mode of BLE is based on non connectable undirected advertisements. In BLE, the 2.4 GHz band is divided into 40 frequency channels of 2 MHz, three of which are dedicated for advertisements. The advertisement channels are the channels 37 (at 2402 MHz), 38 (at 2426 MHz) and 39 (at 2480 MHz). On each transmission event, the wearable sensor transmits an advertisement frame of up to 39 bytes. Part of these 39 bytes are used for addressing and other headers. Up to 26 bytes per advertisement are available for the application layer. Each triaxial accelerometer sample is 6 bytes (12-bit resolution); therefore, a BLE advertisement can contain up to 4 accelerometer samples. In the remaining 2 bytes, we include a sequence number and the voltage of the battery storage unit.

The simplicity of the connectionless mode of BLE makes it an ideal choice for residential monitoring. Its advantages can be summarised as follows. First, the advertisement channels are carefully selected to fall in between the popular IEEE 802.11 channels 1, 6 and 11. Since these WiFi channels are most commonly used [27][28], the interference between WiFi and BLE is mitigated. Most importantly, when the user is moving, handovers to other *Observers* are seamless, quick and without overhead. Lastly, the minimalistic design of connectionless BLE translates to low overhead and direct benefits on energy consumption. In short, there are no transmissions of acknowledgements, no idle listening overheads for receiving data, no connection-establishment overheads. The main weakness of connectionless BLE is packet loss due to the lack of retransmissions. Related works have investigated several techniques that can be employed to mitigate packet loss in connectionless BLE [29][30]. In outdoors scenarios, connectionless BLE can be used along with a smart phone operating as a receiver. It should be noted that connection-oriented BLE is fundamentally compatible with the proposed system architecture; although the overall energy consumption is expected to be higher.

B. Smart Infrastructure

The smart infrastructure consists of a set of receiver units that are responsible for relaying the accelerometer data to a local database or the cloud. The receiving functionality, implemented on a Raspberry Pi micro-computer, incorporates

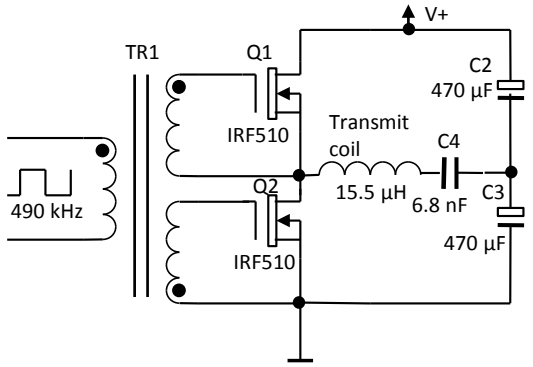

Fig. 5. Half-bridge coil driver - outline circuit.

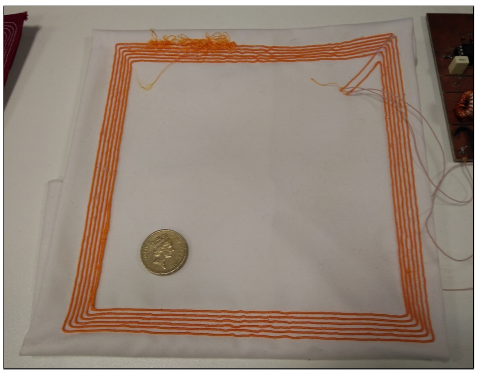

Fig. 6. The prototype textile transmit coil.

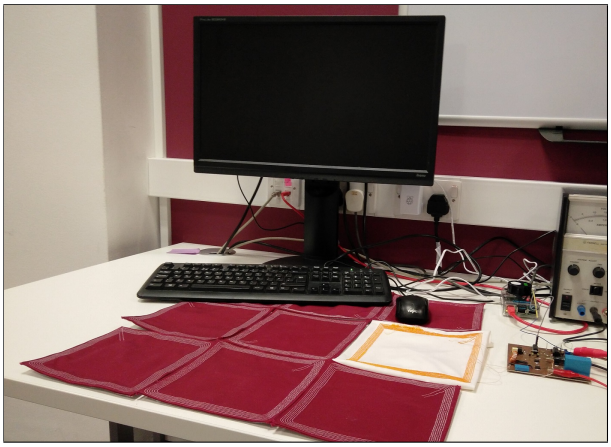

Fig. 7. The smart charging surface prototype with a matrix of 9 textile coils (the transmit coil and 8 repeat coils) deployed on a computer desk.

the set of packet loss mitigation techniques proposed in [30] to guarantee full-house coverage on top of an off-the-shelf BLE radio. In addition, the receiver units are co-located with smart inductive charging surfaces, strategically positioned in areas of the house where the user is expected to spend a considerable amount of time during their daily routine.

The transmit coil is operated in series resonance, driven at 490 KHz by a half-bridge Class-D driver circuit, as shown in outline form in Fig. 5. C2 and C3 maintain one end of the tuning capacitor C4 at mid-rail potential, *i.e.* V+/2, whilst MOSFETs Q1 and Q2 switch on alternately, applying a square-wave voltage to the resonant circuit. Since the series circuit has a high impedance at harmonic frequencies but is resistive at the fundamental frequency, this results in a sinusoidal transmit coil current waveform. The voltage applied to the half-bridge, V+ in Fig. 5, is adjusted to give the required driver current, which for these tests was 2 A RMS.

The coils making up the charging area are flexible, a feature which allows them to accommodate curved surfaces or even to be incorporated into soft furnishings, for instance into the arms of a chair to power a wrist-worn device, or into a chair back, to power a device integrated into a garment. The coils are square (130×130 mm) and are constructed using Litz wire embroidered onto a light canvas sheet as seen in Fig. 6, which shows a photograph of the prototype transmit coil. The coil is wound with six turns of 81/0.04 Litz wire and has an inductance of 15.5 μH. It is tuned to series resonance at 490 KHz using a 6.8 nF film capacitor. The repeater coils are identical except for the use of 36/0.04 Litz wire for greater flexibility; they are parallel tuned using the same 6.8 nF capacitor incorporated within a pocket on the canvas backing. Eight repeater coils are placed around the transmit coil to form a 3×3 matrix, as shown in Fig. 7. Magnetic flux loops around the edges of the transmit coil link with the turns of the surrounding repeater coils, each one relaying flux to its neighbour. In this way, all the coils are excited to resonance, providing a carpet of alternating magnetic flux.

The receiver unit activates and deactivates the inductive charging surface based on the voltage level received from the wearable, *i.e.*, the supercapacitor voltage, and the RSSI. The RSSI is used to determine the proximity of the wearable to the inductive charging surface, whilst the voltage level determines whether the wearable needs recharging. Three thresholds are defined: one RSSI threshold and two voltage thresholds. When the RSSI is above the RSSI threshold, the wearable is assumed to be in close proximity. When packets are received but the RSSI is below the threshold, the wearable is assumed to be far from the charging surface. Moreover, when no packets are received by the particular receiver unit, yet packets are received by other receiver units, the wearable is again assumed to be far from the particular charging surface. On the other hand, when no packets are received at all, the system is in an ambiguous state where the wearable is either too far from the whole infrastructure or the energy storage unit of the wearable is depleted. In the latter state the charging surface is activated periodically for a predetermined window. When the wearable is in close proximity to the charging surface, the transmitted voltage from the wearable's energy storage unit determines whether the charging surface gets activated. The transmit-coil driver is turned on when the received voltage is below a lower threshold, and off when it is above an upper threshold. This establishes a hysteresis band between which no change takes place, preventing oscillation of the driver on-off signal as the

switching threshold is approached. Moreover, the charging surface gets deactivated when the wearable loses its proximity to it. To avoid fluctuations, a fixed delay is induced between decision and actuation in the active to inactive state transition. All thresholds are determined empirically as they depend on the employed antennas and on the voltage characteristics of the employed energy storage unit.

IV. System Evaluation

The system evaluation begins with providing measurements on the power consumption of the wearable for various configurations (*e.g.* sampling frequency). It continues with the characterisation of the energy harvesting potential of an inductive charging surface, including experiments where users were asked to use the proposed system. The requirements for energy neutral operation are, then, identified in terms of how frequently the user needs to use their computer for their wearable to be energy neutral. In addition, the evaluation includes measurements demonstrating that the system adheres to health regulations regarding electromagnetic exposure.

A. Power Consumption of Wearable Sensor

Mitigating the power consumption of wearable sensors constitutes a key challenge for providing energy neutral operation. This requires the employment of energy conscious practices in the design of both the wearable platform and its firmware. In this section, we evaluate the power consumption of our wearable sensor for various system configurations, which include the sampling frequency and transmission power. The power consumption is calculated by measuring the voltage drop across a resistor in series with the positive side of the power supply.

We begin by measuring the continuous power consumption of the wearable system. When in sleep mode, the system consumes 8.2 μW. The accelerometer contributes an additional 3 μW (maximum consumption at 50 Hz sampling frequency). Periodically, the system moves off the sleeping state to transfer 4 acceleration samples from the accelerometer to the MCU, format them into a BLE advertisement and broadcast them using the BLE radio. Fig. 8 plots the total energy consumed for a transmission event for various levels of the transmission power. It can be observed that at the maximum transmission power level, 4 dBm, the system consumes 61.7 μJ for a transmission event. Lower transmission power levels trade coverage for energy savings. Significant savings can be achieved at up to -4 dBm, where the system consumes 41.1 μJ for a transmission event (33% reduction). Below that, energy savings are minimal, but the wireless coverage is significantly compromised.

The overall long-term average power consumption of the system can be approximated by the following equation:

$$P_C = P_{cont} + \frac{f}{4} E_{BLE}(P_{tx}) \quad (2)$$

where P_{cont} is the continuous power consumption of the system including the accelerometer; $E_{BLE}(P_{tx})$ is the energy consumption of a transmission event at transmission power of P_{tx} given by Fig. 8; and f is the sampling frequency of the accelerometer. Fig. 9 plots the long-term average power consumption of the wearable sensor for the three highest transmission power levels and for various acceleration sampling frequencies. For instance, at 7.8 Hz (*i.e.* 128 ms sampling period) the overall average power consumption is approximately 135 μW. We refer the reader to [31] and [32] for experiments on how the sampling frequency affects the activity recognition performance and how the transmission power affects the wireless coverage respectively. In this configuration the employed 330 mF supercapacitor offers an autonomy of 5.2 hours. It should be noted that the selection of the capacitance of the energy storage unit is meant to facilitate quick experiments. In practice, a supercapacitor, sized for 24 hours of autonomy, is generally recommended.

The role of the inductive charging subsystem is to passively harvest sufficient energy to meet such application requirements, as the user routinely performs everyday activities.

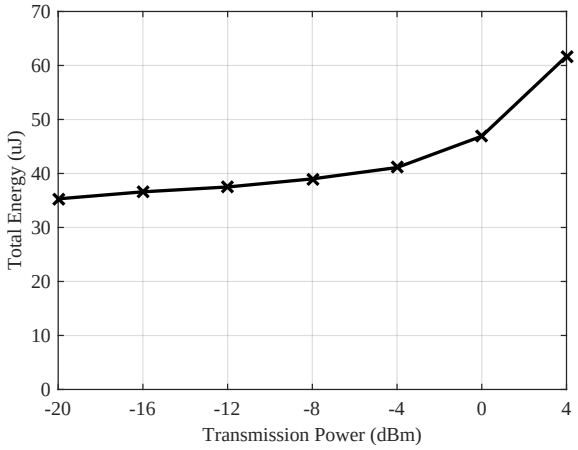

Fig. 8. Energy consumed during an advertising event.

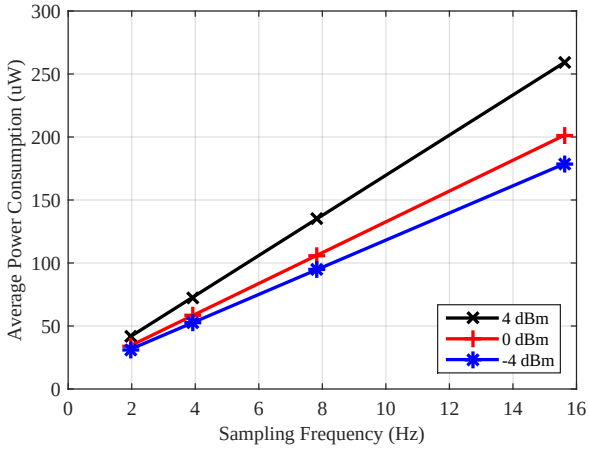

Fig. 9. Long-term average power consumption of the wearable sensor for various sampling frequencies and transmission power levels.

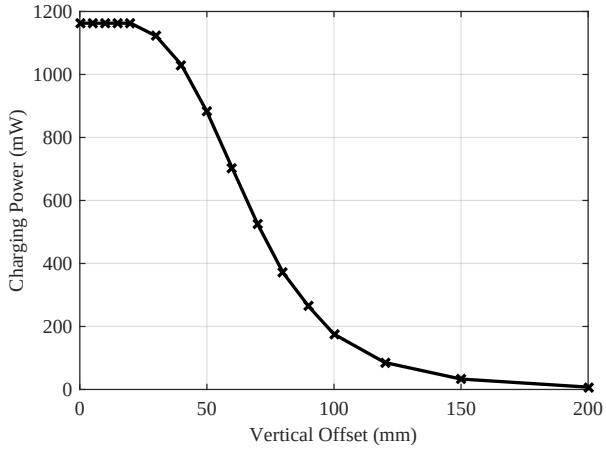

Fig. 10. Charging power against the vertical offset from the centre of the transmit coil.

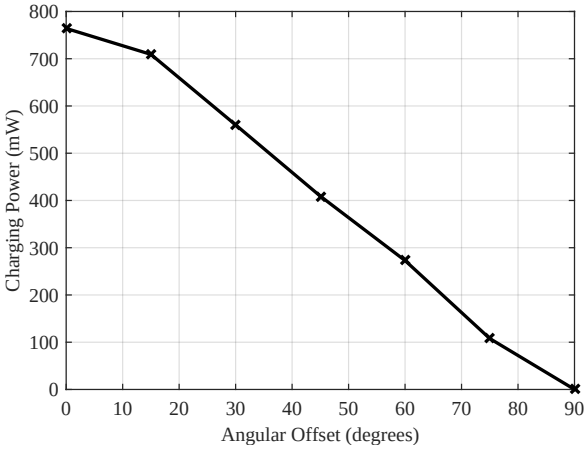

Fig. 12. Charging power against the angular offset from a horizontal orientation on top of the centre of the transmit coil at a height of 65 mm.

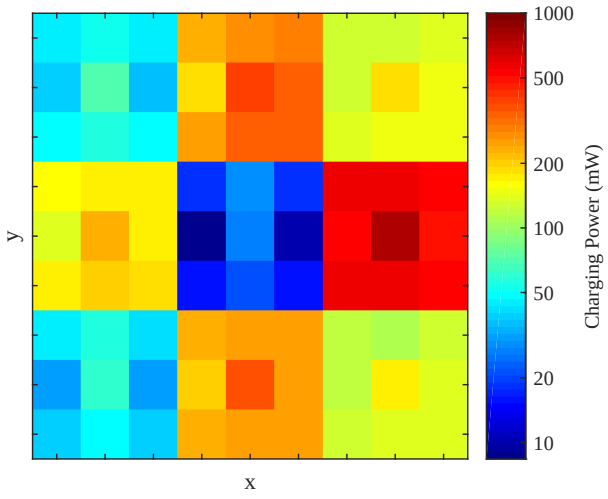

Fig. 11. Charging power map across the grid of coils at a vertical offset of 65 mm. Each square corresponds to an area of 57×57 mm. The transmit coil is positioned in the middle of the third column.

B. Evaluation of the Inductive Charging Surface

The charging power of the inductive charging surface heavily depends on the position and the orientation of the wearable sensor. The evaluation of the charging subsystem begins with the quantification of the charging power for various displacements and ends with the identification of the average charging power when the system is being used.

Fig. 10 plots the charging power against vertical offset from the centre of the transmit coil, with the wearable sensor parallel to the coil. It is seen that charging power drops sharply with vertical displacement, having fallen to approximately 600 mW at 65 mm, close to the height of the wearable above the surface when wrist-worn; yet at 200 mm, 7.5 mW was measured, sufficient to power the wearable and trickle-charge the supercapacitor. Fig. 11 plots the charging power along the 3×3 grid of coils at a constant height of 65 mm. Again, the wearable sensor is parallel to the coils. The grid corresponds to the deployment shown in Fig. 7 where the transmit coil is positioned in the middle of the third column of the 3×3 grid. Each of the 9 coils is split into a 3×3 matrix with each small square corresponding to an area of 57×57 mm. As the colour map shows, the repeater coils spread the available charging power over the whole area of the mat, if somewhat unevenly, the lowest power reading being in the centre mat; but even here 10 mW is available. The uneven nature of the power distribution is due to cancellation effects in the propagation of the magnetic flux from different paths in the coil matrix; this will be better understood when a full analysis of the magnetic coupling throughout the coil matrix has been carried out. Fig. 12 plots the charging power against the angular rotation of the wearable sensor, which is positioned 65 mm above the centre of the transmit coil. An approximately linear behaviour can be observed yielding zero charging power when the coils are orthogonal.

Although a very high charging power can be achieved in the best case scenario, in a real scenario the wearable sensor is worn by the user who is constantly moving. In the next experiment, we attempt to identify the average charging power of the wearable sensor whilst the user engages in a typical everyday activity. For this purpose, we deployed a prototype charging surface on a computer desk, as shown in Fig. 7. A total number of 8 users were instructed to casually use the computer while wearing the wearable sensor on the wrist of their dominant hand. Fig. 13 plots their respective average harvested power. The conducted experiments yield an overall average charging power of $\mu = 42.7$ mW ($\sigma = 14.6$ mW).

C. Requirements for Energy Neutral Operation

The wearable system is energy neutral if, over a time period that its energy buffers can support, the consumed energy is less than or equal to the harvested energy [13]. In the system presented in this paper, the wearable device is passively charged

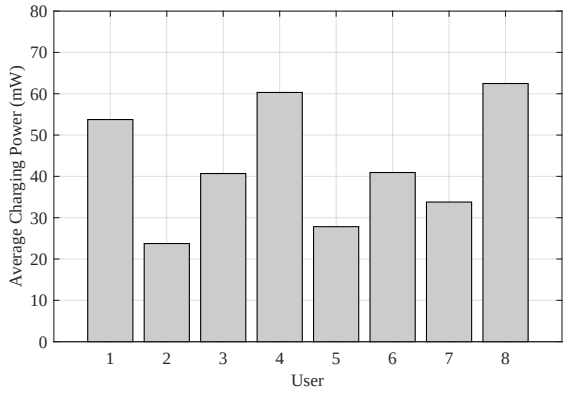

Fig. 13. Long-term average charging power while 8 different subjects routinely use their computer ($\mu = 42.7$ mW, $\sigma = 14.6$ mW).

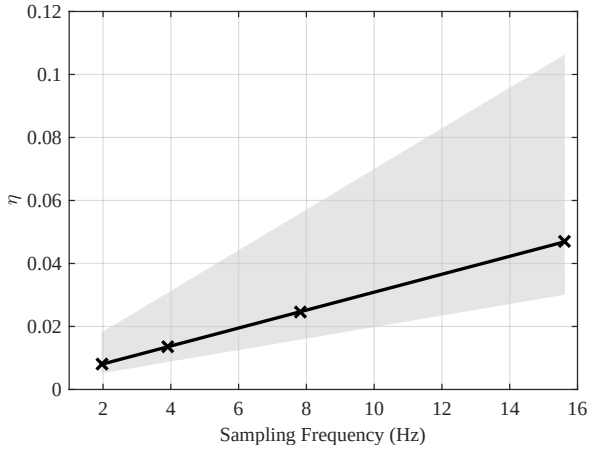

Fig. 14. The sustainability ratio, η, identifies the limit of how frequently the user needs to engage in the everyday activities that passively charge the wearable in order to ensure ENO. The estimations are based on the experiments with 8 users ($P_H = 42.7$). The shared area corresponds to 90% confidence intervals.

when the user performs daily activities. The requirements for energy neutrality can, therefore, be expressed as the ratio of the time the user performs such routine activities (T_A) over the autonomy the harvested energy provided by performing these activities can offer (T_L). We define this ratio as η. Assuming sufficient energy storage capacity, η can be expressed as the ratio of the long-term average power consumption (P_c) over the long-term average harvested power (P_H) during a passive charging event:

$$\eta = \frac{T_H}{T_C} = \frac{P_C}{P_H} \ . \tag{3}$$

In other words, the ratio η identifies how frequently the users need to engage to the everyday activities that are passively charging their wearable in order to ensure ENO.

In Fig. 14, we plot the sustainability ratio η for various sampling frequencies (f) and for $P_{tx} = 0$ dBm. The estimations are based on the experiments with 8 users ($P_H = 42.7$ mW) presented in the previous section. The shaded area corresponds to 90% confidence intervals on the average charging power. For instance, at 7.8 Hz (*i.e.* 128 ms sampling period) η is equal to 0.025. As a result, assuming the supercapacitor is sized to provide autonomy for 24 hours, as long as the wearers use their computer for more than 36 minutes per day, the wearable is energy neutral and, therefore, maintenance-free.

Concluding this section, it is important to note that additional smart charging surfaces that associate with other everyday activities (*e.g.* dining, watching TV) share the requirements for passive charging amongst multiple activities. Therefore, deploying multiple smart charging surfaces not only improves wireless coverage but also loosens the per-activity requirements for sustainable operation.

D. Adherence to Health Regulations

For operation in Europe, an IPT system must meet the ICNIRP (International Commission on Non-Ionizing Radiation Protection) guidelines [33] regarding electromagnetic exposure. For operation between 100 KHz and 10 MHz, [33] gives specific absorption rates (SAR) for various parts of the body, including 0.08 W/kg forthe whole body, 2 W/kg for the head and trunk, and 4 W/kg for the limbs. To calculate SAR, tissue current density J is first found using the following equation as specified in [33]:

$$J = \pi r \sigma F D \ , \tag{4}$$

where r is the coil radius, σ is tissue conductivity (0.446 S/m at 500 KHz), F is the frequency and B is the RMS coil flux density. The magnetic field is most intense above the transmit coil and we perform calculations assuming full contact with the surface of this coil, giving a value of $J = 13.6$ A/m^2. SAR is calculated using the following equation as specified in [34]:

$$SAR = \frac{J^2}{\sigma \rho} \ , \tag{5}$$

where ρ is tissue density (1060 kg/m^3). This yields a figure of 0.39 W/kg, which falls well within the limits for limbs, but also for the whole body considering the proximity of a person to the coils when using this system.

V. Conclusion

The maintenance overhead of regular battery recharging limits the applicability of wearable sensors for medical applications. In this paper, we present a maintenance-free wearable sensing system. The system is composed of a BLE-enabled activity sensing platform that yields a long-term average power consumption of 135 uW at a sampling frequency of approximately 8 Hz. The wearable sensor broadcasts acceleration data to a set of receiver units. Each receiver unit is co-located with a smart charging surface that is based on an experimental IPT system that enables wireless charging over an extended area that expands laterally using textile repeater coils and vertically up to 20 cm. By integrating the textile coils on frequently-used rigid or soft furniture, the system provides an unobtrusive charging solution that passively charges the wearable without

user intervention. Measurements on a prototype implementation of the system on a computer desk suggest that being in the vicinity of the charging surface charges the energy storage unit of the wearable sensor at rates that are orders of magnitude above the power consumption figures (1 mW to 1 W depending on the exact position and orientation with respect to the primary transmit coil). Regular computer usage yields an average charging power of 42.7 mW; suggesting that with an appropriately sized energy storage unit, 36 minutes of daily computer usage is on average sufficient to maintain the wearable sensor energy neutral.

As future work, we plan to quantify the trade-off associated with the RSSI threshold for determining the proximity of the user to the charging surface: a tighter threshold would reduce the average charging rate, whereas a looser threshold would compromise the energy-efficiency on the infrastructure side. Moreover, we plan to further analyse the magnetic coupling throughout the coil matrix in order to identify the propagation properties of the magnetic flux.

ACKNOWLEDGEMENTS

This work was performed under the SPHERE IRC funded by the UK Engineering and Physical Sciences Research Council (EPSRC), Grant EP/K031910/1. We would also like to thank all the SPHERE researchers who contributed in the development of the technologies used in this work.

REFERENCES

[1] M. Haak, A. Fänge, S. Iwarsson, and S. D. Ivanoff, "Home as a signification of independence and autonomy: experiences among very old Swedish people." *Scand. J. Occup. Ther.*, vol. 14, no. 1, pp. 16–24, 2007.

[2] Royal College of Nursing, "Children and young peoples mental health every nurses business: RCN guidance for nursing staff," 2014.

[3] M. Chan, D. Estve, C. Escriba, and E. Campo, "A review of smart homespresent state and future challenges," *Computer Methods and Programs in Biomedicine*, vol. 91, no. 1, pp. 55 – 81, 2008.

[4] X. Fafoutis, E. Tsimbalo, E. Mellios, G. Hilton, R. Piechocki, and I. Craddock, "A residential maintenance-free long-term activity monitoring system for healthcare applications," *EURASIP Journal on Wireless Communications and Networking*, vol. 2016, no. 31, Jan. 2016.

[5] T. J. M. Kooiman, M. L. Dontje, S. R. Sprenger, W. P. Krijnen, C. P. van der Schans, and M. de Groot, "Reliability and validity of ten consumer activity trackers." *BMC Sports Sci. Med. Rehabil.*, vol. 7, no. 1, p. 24, Jan. 2015.

[6] M. Chan, D. Estève, J.-Y. Fourniols, C. Escriba, and E. Campo, "Smart wearable systems: Current status and future challenges," *Artificial Intell. in Medicine*, vol. 56, no. 3, pp. 137 – 156, 2012.

[7] S. Sudevalayam and P. Kulkarni, "Energy harvesting sensor nodes: Survey and implications," *Communications Surveys Tutorials, IEEE*, vol. 13, no. 3, pp. 443–461, Third 2011.

[8] M. Gorlatova, A. Wallwater, and G. Zussman, "Networking low-power energy harvesting devices: Measurements and algorithms," in *Proc. IEEE Int. Conf. on Comput. Commun. (INFOCOM)*, April 2011, pp. 1602–1610.

[9] M. Gorlatova, J. Sarik, G. Grebla, M. Cong, I. Kymissis, and G. Zussman, "Movers and shakers: Kinetic energy harvesting for the internet of things," in *Proc. ACM Int. Conf. on Measurement and Modeling of Computer Systems (SIGMETRICS)*. ACM, 2014, pp. 407–419.

[10] S. Hui, "Planar Wireless Charging Technology for Portable Electronic Products and Qi," *Proceedings of the IEEE*, vol. 101, no. 6, pp. 1290–1301, June 2013.

[11] S. Chalasani and J. Conrad, "A survey of energy harvesting sources for embedded systems," in *Southeastcon, 2008. IEEE*, April 2008, pp. 442–447.

[12] C. Valenta and G. Durgin, "Harvesting wireless power: Survey of energy-harvester conversion efficiency in far-field, wireless power transfer systems," *Microwave Magazine, IEEE*, vol. 15, no. 4, pp. 108–120, June 2014.

[13] A. Kansal, J. Hsu, S. Zahedi, and M. B. Srivastava, "Power management in energy harvesting sensor networks," *ACM Trans. Embed. Comput. Syst.*, vol. 6, no. 4, Sep. 2007.

[14] N. Tesla, *My Inventions: The Autobiography of Nikola Tesla*. Experimenter Publishing Company Inc., 1919.

[15] M. Budhia, G. Covic, and J. Boys, "Design and Optimization of Circular Magnetic Structures for Lumped Inductive Power Transfer Systems," *IEEE Trans. Power Electronics*, vol. 26, no. 11, pp. 3096–3108, Nov 2011.

[16] K. Silay, C. Dehollaini, and M. Declercq, "Inductive power link for a wireless cortical implant with biocompatible packaging," in *IEEE Sensors*, Nov 2010, pp. 94–98.

[17] L. Theogarajan, "A Low-Power Fully Implantable 15-Channel Retinal Stimulator Chip," *IEEE J. Solid-State Circuits*, vol. 43, no. 10, pp. 2322–2337, Oct 2008.

[18] O. Jonah, S. Georgakopoulos, and M. Tentzeris, "Wireless power transfer to mobile wearable device via resonance magnetic," in *Proc. 14th IEEE Annul. Wireless and Microwave Technology Conf. (WAMICON)*, April 2013, pp. 1–3.

[19] M. Catrysse, R. Puers, C. Hertleer, L. V. Langenhove, H. van Egmond, and D. Matthys, "Towards the integration of textile sensors in a wireless monitoring suit," *Sensors and Actuators A: Physical*, vol. 114, no. 23, pp. 302 – 311, 2004, selected papers from Transducers 03.

[20] S. Lee, J. Yoo, H. Kim, and H.-J. Yoo, "A dynamic real-time capacitor compensated inductive coupling transceiver for wearable body sensor network," in *VLSI Circuits, 2009 Symposium on*, June 2009, pp. 42–43.

[21] W. Chen, C. Sonntag, F. Boesten, S. B. Oetomo, and L. Feijs, "A design of power supply for neonatal monitoring with wearable sensors," *J. Ambient Intell. Smart Environ.*, vol. 1, no. 2, pp. 185–196, Apr. 2009.

[22] L. Clare, P. Worgan, B. Stark, S.-E. Adami, and D. Coyle, "Influence of exposure guidelines on the design of on-body inductive power transfer," in *Proc. IEEE Wireless Power Transfer Conf. (WPTC)*, May 2015, pp. 1–4.

[23] P. Worgan, L. Clare, P. Proynov, B. Stark, and D. Coyle, "Inductive Power Transfer for On-body Sensors. Defining a design space for safe, wirelessly powered on-body health sensors." in *Proc 9th Int. Conf. on Pervasive Comput. Technologies for Healthcare*, 2015.

[24] Bluetooth SIG, "Specification of the Bluetooth System - Covered Core Package version: 4.0," 2010.

[25] Nordic Semi., "nRF51822 - Product Specification v2.0," 2013.

[26] S. Burrow and L. Clare, "Open-loop power conditioning for vibration energy harvesters," *Electronics Letters*, vol. 45, no. 19, pp. 999–1000, September 2009.

[27] G. Valadon, F. Le Goff, and C. Berger, "A Practical Characterization of 802.11 Access Points in Paris," in *Proc. 5th Adv. Int. Conf. Telecomm. (AICT)*, 2009, pp. 220–225.

[28] A. Akella, G. Judd, S. Seshan, and P. Steenkiste, "Self-management in Chaotic Wireless Deployments," in *Proc. 11th An. Int. Conf. on Mobile Comp. and Networking (MobiCom)*. ACM, 2005, pp. 185–199.

[29] E. Tsimbalo, X. Fafoutis, and R. Piechocki, "Fix It, Dont Bin It! - CRC Error Correction in Bluetooth Low Energy," in *Proc. 2nd IEEE World Forum on Internet of Things (WF-IoT)*, 2015.

[30] E. Tsimbalo, X. Fafoutis, E. Mellios, M. Haghighi, B. Tan, G. Hilton, R. Piechocki, and I. Craddock, "Mitigating Packet Loss in Connectionless Bluetooth Low Energy," in *Proc. 2nd IEEE World Forum on Internet of Things (WF-IoT)*, 2015.

[31] U. Maurer, A. Smailagic, D. Siewiorek, and M. Deisher, "Activity recognition and monitoring using multiple sensors on different body positions," in *Int. Workshop on Wearable and Implantable Body Sensor Networks (BSN)*, 2006.

[32] M. W. Abdullah, X. Fafoutis, E. Mellios, M. Klemm, and G. Hilton, "Investigation into Off-Body Links for Wrist Mounted Antennas in Bluetooth Systems," in *Proc. Loughborough Antennas and Propagation Conf. (LAPC)*, 2015.

[33] International Commission on Non-Ionizing Radiation Protection, "ICNIRP guidelines for limiting exposure to time-varying electric and magnetic fields," pp. 494–522, 1998.

[34] World Health Organisation, "EHC 137, Chapter 5, 5.2.1. Magnetic Fields," 1993.